

## A SYMMETRICAL DUAL-BAND TERAHERTZ META-MATERIAL WITH CRUCIFORM AND SQUARE LOOPS

B. Li<sup>1, \*</sup>, L. X. He<sup>2</sup>, Y. Z. Yin<sup>1</sup>, W. Y. Guo<sup>2, 3</sup>, and X. W. Sun<sup>2</sup>

<sup>1</sup>National Laboratory of Antennas and Microwave Technology, Xidian University, Xi'an, Shaanxi 710071, China

<sup>2</sup>Key Laboratory of Terahertz Technology, Shanghai Institute of Microsystem and Information Technology, Shanghai 200050, China

<sup>3</sup>Graduate University of Chinese Academy of Sciences, Beijing 100049, China

**Abstract**—A symmetrical terahertz metamaterial for dual-band operation is designed and fabricated. The proposed metamaterial is composed of periodically arranged cruciform and square metal loops. Due to the symmetrical structure, this metamaterial is insensitive with the polarization of the incident wave. Transmission and reflection characteristics of the proposed structure are simulated using Ansoft HFSS, and the negative permittivity is figured out in 378–500 GHz and 626–677 GHz bands. The designed sample is fabricated on a gallium arsenide layer, and experiments are performed in Terahertz Time-Domain Spectroscopy. The experimental results agree well with the simulations.

### 1. INTRODUCTION

Metamaterials (MMs) are engineered materials which show negative permittivity and/or negative permeability composites with embedded sub-wavelength metallic structures. Materials with simultaneously negative permittivity and magnetic permeability were not accessible in naturally occurring materials, while they were theoretically considered by Veselago in 1968 [1]. The first MM was theoretically analyzed by Pendry [2] who noticed that a microstructure built of nonmagnetic

---

*Received 13 September 2012, Accepted 15 October 2012, Scheduled 19 October 2012*

\* Corresponding author: Biao Li (mwbiaoli@163.com).

conducting split-ring resonators (SRR) can be tuned to negative values of magnetic permeability. Smith made the first prototype structures of double negative (DNG) material [3]. From then on, various metallic artificial structures, such as the double split-ring resonators (DSRRs) [4], spiral resonators (SRs) [5], S-shaped resonators [6, 7], V-shaped resonators [8] and  $\Omega$ -shaped resonators [9] were proposed in pursuing the negative values for the real part of effective permeability and/or permittivity over narrow spectral bands. Most early researches in MM operated in the microwave regime, while the design and applications in terahertz (THz) regime have attracted great attention [9–12]. Recently, many dual-band and broad-band MM have been reported [10–12], while the designs in these reports are polarization sensitive. In order to conquer this problem, many new approaches have been presented [13–15]. The three-dimensional MM tube which is made by rolling up two-dimensional planar MM is insensitive with the polarization of the incident wave due to its axial symmetry [13]. And a modified FMM with holes of square shape can also make the structure polarization independent [14].

In this paper, we present a THz MM with dual-band operation based on a novel sub-wavelength structure. It is found that negative permittivity in 378–500 GHz and 626–677 GHz bands can be obtained. Due to the symmetrical structure, this MM is insensitive with the polarization of the incident wave. As shown in Fig. 1, the proposed electrical resonator is structured by periodically arranged cruciform

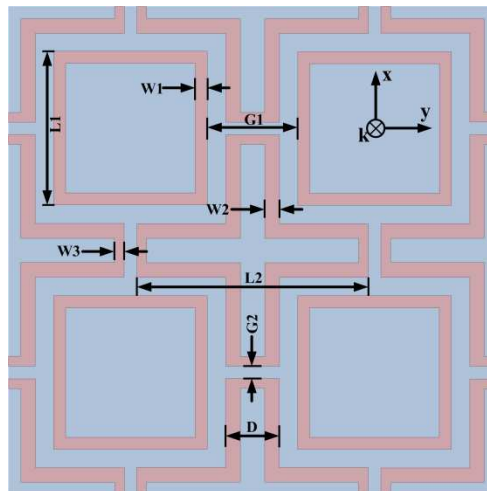


**Figure 1.** Geometry and parameters of the proposed MM unit cell.

and square loops and the parameters are  $L1 = 63 \mu\text{m}$ ,  $L2 = 95 \mu\text{m}$ ,  $W1 = 5 \mu\text{m}$ ,  $W2 = 5 \mu\text{m}$ ,  $W3 = 4 \mu\text{m}$ ,  $G1 = 37 \mu\text{m}$ ,  $G2 = 5 \mu\text{m}$  and  $D = 22 \mu\text{m}$ .

## 2. DESIGN AND SIMULATION

The proposed structures are simulated and optimized by using Ansoft's High Frequency Structure Simulator (HFSS) tools, which is based on the finite element method. The MM model is designed on a 20- $\mu\text{m}$ -thick gallium arsenide (GaAs) layer with a real permittivity of 12.9 and a loss tangent of 0.006, and the metal layer is gold with the thickness of 0.3  $\mu\text{m}$ . The geometrical structure of the proposed MM unit cell is described in Fig. 1. The incident wave is in the  $z$ -direction, and the polarization is parallel with the  $y$ -direction.

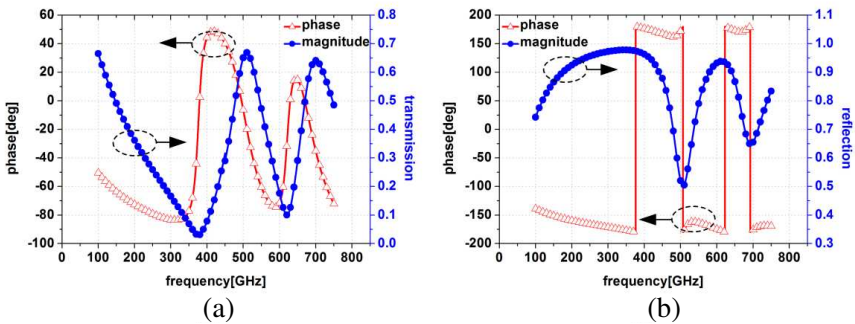


**Figure 2.** Simulated (a) transmission and (b) reflection parameters of the proposed MM with the polarization in  $y$ -direction.

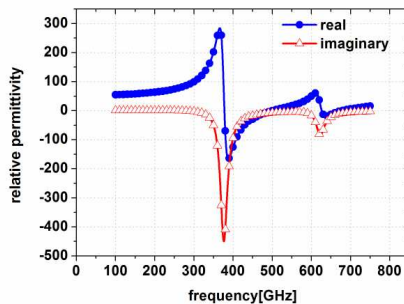


**Figure 3.** Calculated relative permittivity of the proposed MM.

The simulated magnitude and phase results for transmission and reflection parameters of the proposed MM are shown in Figs. 2(a) and (b). Because of the symmetry of the structure, we can get almost the same result when the polarization is parallel with the  $x$ -direction, and the result is omitted in Fig. 2. The transmitted (reflected) wave has two stop-band (pass-band) regions around the resonant frequencies, and we can claim that this structure almost perfectly reflects the electromagnetic (EM) wave in the transmission stop-band regions.

By using the methods and models mentioned in [16, 17], the effective medium parameters are calculated. The basic equations used to determine the  $\varepsilon_r$  and  $\mu_r$  are shown below:

$$\varepsilon_r \approx \frac{2}{jk_0d} \frac{1 - v_1}{1 + v_1} \quad (1)$$

$$\mu_r \approx \frac{2}{jk_0d} \frac{1 - v_2}{1 + v_2} \quad (2)$$

where  $v_1 = S_{21} + S_{11}$ ,  $v_2 = S_{21} - S_{11}$ ,  $k = \omega/c$ ,  $\omega$  is Radian frequency,  $d$  the slab thickness, and  $c$  the speed of light.

As is illustrated in Fig. 3, the real part of relative permittivity shows negative values over the bands 378–500 GHz and 626–677 GHz. Thus a dual-band THz MM based on the proposed sub-wavelength structure is realized. In this paper,  $e^{(+j\omega t)}$  is used as the time convention, and the negative imaginary permittivity implies loss.

To clearly present the generation of the two resonances, the MM with only the cruciform loops and the square loops are simulated for comparison, as shown in Figs. 4(a) and (b). The magnitude results for transmission of the three models are demonstrated in Fig. 5(a),

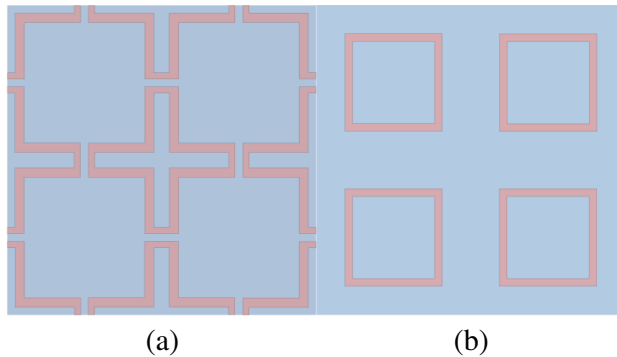


**Figure 4.** Structures with only (a) cruciform loops and (b) square loops.

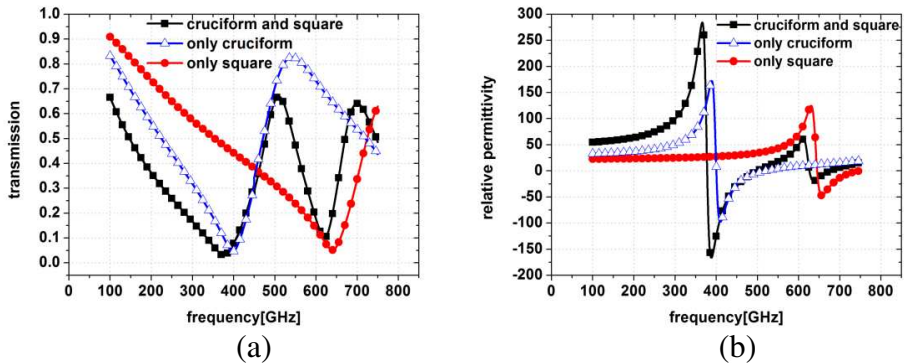


**Figure 5.** (a) Transmission and (b) relative permittivities of the three structures.

from which, we can see that cruciform loops and square loops generate the lower and higher bands separately. The real part of the relative permittivities of the three models is also shown in Fig. 5(b), which is calculated using the method above.

As the common viewpoint, the LC equivalent circuit is the cause of the electromagnetic resonance, no matter what geometry configurations they are. The inductance  $L$  comes from induced currents and a gap or split stands for the capacitance  $C$ . The electric field and the surface current distribution of metal structure at the two resonance frequency is shown in Fig. 6 (The polarization of the incident wave is parallel with the  $y$ -direction). It is demonstrated that the electric field is mainly distributed in the gap between the neighbor cruciform loops along the polarized direction (gap I in Fig. 6(a)) at the lower band (370 GHz), while in the gap between the square loops (gap II in Fig. 6(b)) at the higher band (590 GHz). These gaps act as the capacitance  $C$ , and the metallic lines stands for the inductance  $L$  generated by induced current shown in Figs. 6(c) and (d). Compared with the resonances of the individual single-resonant particles, there is a modest frequency shift for both the two resonant frequencies of the dual-resonant MM, which is expected from the coupling of these resonators. The resonance is mainly caused by the cruciform loops at the lower band. Meanwhile there are induced currents on the square loops. At the higher band, the square loops are resonant, and the cruciform loops also have induced currents. The coupling electric field also existed between the two resonators.

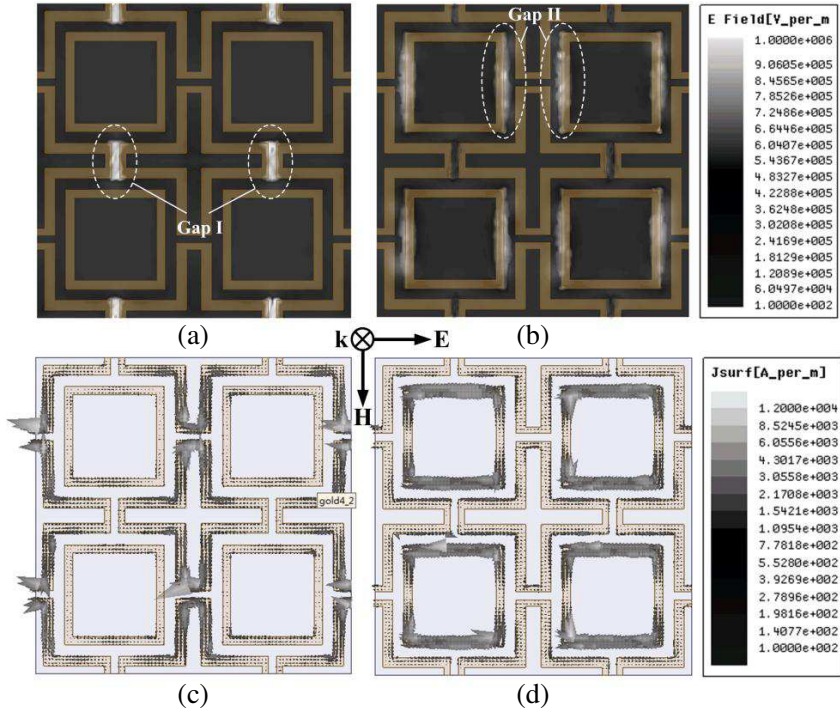


**Figure 6.** Electric field and current distribution of the proposed unit cell. Electric field at (a) 370 GHz and (b) 590 GHz, current distribution at (c) 370 GHz and (d) 590 GHz.

### 3. FABRICATION AND EXPERIMENT

To verify the design and simulation results, the periodic metallic array of the proposed sub-wavelength structures are fabricated on the 350- $\mu\text{m}$ -thick gallium arsenide (GaAs) substrate using magnetron sputtering method. Fig. 7 shows the photograph of the fabricated sample under a microscope. The periodic metallic array is composed of titanium (Ti), platinum (Pt) and gold (Au) layers (the thicknesses of Ti/Pt/Au: 20/20/300 nm). The Ti layer is used to ensure a good adhesion to the substrate, and the Pt layer placed between Ti and Au is helpful to prevent the possible intermetallic diffusion. Experiments of the designed sample are performed in Terahertz Time-Domain Spectroscopy (THz-TDS) equipment at room temperature in a dry nitrogen atmosphere. When the THz wave propagates at normal incidence ( $z$ -direction), the experimental sample behaves as a dual-band THz MM.

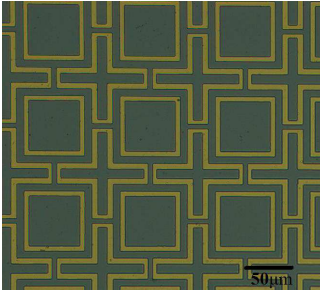


**Figure 7.** Photograph of the fabricated MM sample under a microscope.

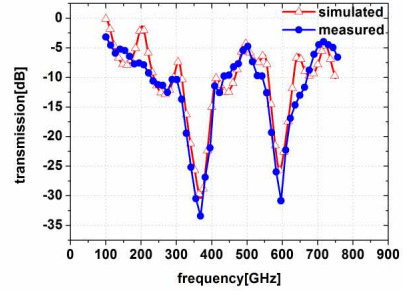


**Figure 8.** Measured and Simulated transmissions of the experimental sample.

The measured and simulated transmissions of this structure are plotted in Fig. 8. Fourier transform is used to calculate the frequency-domain results from the time-domain signal in the THz-TDS experiments, and portions of the signal caused by Fresnel reflections are removed. It can be seen that dual-band near 370 GHz and 590 GHz with the transmissions below  $-20$  dB is obtained. Between the two resonances, there is a peak at 490 GHz with a transmission higher than 45%. Good agreement between the measured and simulated results is achieved.

#### 4. CONCLUSIONS

In summary, the design, fabrication and experiment of a symmetrical dual-band THz MM are presented. The proposed novel sub-wavelength structure intensely resonates at 370 GHz and 590 GHz. The fabricated metamaterial sample is measured using the THz-TDS equipment, and the results show good agreement with the simulations. Based on the electric-field-coupling, negative values of permittivity in bands 378–500 GHz and 626–677 GHz are achieved, which has potential applications for the multi-band applications in THz regime.

#### ACKNOWLEDGMENT

This work was supported by the National Basic Research Program under Grant 2009CB320207 of China.

## REFERENCES

1. Veselago, V. G., "The electrodynamics of substances with simultaneously negative values of permittivity and permeability," *Sov. Phys. Usp.*, Vol. 10, No. 4, 509–514, Jan.–Feb. 1968.
2. Pendry, J. B., A. J. Holden, D. J. Robbins, and W. J. Stewart, "Magnetism from conductors and enhanced nonlinear phenomena," *IEEE Trans. Microw. Theory Tech.*, Vol. 47, No. 11, 2075–2084, Nov. 1999.
3. Smith, D. R., W. J. Padilla, D. C. Vier, S. C. Nemat-Nasser, and S. Schultz, "Loop-wire medium for investigating plasmons at microwave frequency," *Phys. Rev. Lett.*, Vol. 84, 4184–4187, 2000.
4. Yen, T. J., W. J. Padilla, N. Fang, D. C. Vier, D. R. Smith, J. B. Pendry, D. N. Basov, and X. Zhang, "Terahertz magnetic response from artificial materials," *Science*, Vol. 303, No. 5663, 1494–1496, Mar. 2004.
5. Baena, J. D., R. Marques, F. Medina, and J. Martel, "Artificial magnetic metamaterial design by using spiral resonators," *Phys. Rev. B*, Vol. 69, 014402(1)–(5), 2004.
6. Wang, D., L. Ran, H. Chen M. Mu, J. A. Kong, and B. I. Wu, "Experimental validation of negative refraction of metamaterial composed of single side paired S-ring resonators," *Appl. Phys. Lett.*, Vol. 90, 254103(1)–(3), 2007.
7. Wu, B.-I., W. Wang, J. Pacheco, X. Chen, T. M. Grzegorzcyk, and J. A. Kong, "A study of using metamaterials as antenna substrate to enhance gain," *Progress In Electromagnetics Research*, Vol. 51, 295–328, 2005.
8. Sabah, C., "Multi-resonant metamaterial design based on concentric V-shaped magnetic resonators," *Journal of Electromagnetic Waves and Applications*, Vol. 26, No. 8–9, 1105–1115, 2012.
9. Gu, J. Q., J. G. Han, X. C. Lu, R. Singh, Z. Tian, Q. R. Xing, and W. L. Zhang, "A close-ring pair terahertz metamaterial resonating at normal incidence," *Optics Express*, Vol. 12, No. 22, 20307–20312, Oct. 2009.
10. Yuan, Y., C. Bingham, T. Tyler, S. Palit, T. H. Hand, and W. J. Padilla, "A dual-resonant terahertz metamaterial based on single-particle electric-field-coupled resonators," *Appl. Phys. Lett.*, Vol. 93, No. 19, 191110, 2008.
11. Yuan, Y., C. Bingham, T. Tyler, S. Palit, T. H. Hand, and W. J. Padilla, "Dual-band planar electric metamaterial in terahertz regime," *Optics Express*, Vol. 16, No. 13, 9746–9752, Jun. 2008.



12. Ekmekci, E. and G. Turhan-Sayan, "Single loop resonator: Dual-band magnetic metamaterial structure," *Electron. Lett.*, Vol. 46, No. 5, Mar. 2010.
13. Chen, Z. C., R. Mohsen, Y. D. Gong, T. C. Chong, and M. H. Hong, "Realization of variable three-dimensional terahertz metamaterial tubes for passive resonance tunability," *Adv. Mater.*, Vol. 24, OP143–OP147, 2012.
14. García-Meca, C., R. Ortuño, F. J. Rodríguez-Fortuño, J. Martí, and A. Martínez, "Double-negative polarization-independent fishnet metamaterial in the visible spectrum," *Opt. Lett.*, Vol. 34, No. 10, 1603–1605, 2009.
15. Zhu, B., Z. Wang, C. Huang, Y. Feng, J. Zhao, and T. Jiang, "Polarization insensitive metamaterial Absorber with wide incident angle," *Progress In Electromagnetics Research*, Vol. 101, 231–239, 2010.
16. Ziolkowski, R. W., "Design, fabrication, and testing of double negative metamaterials," *IEEE Trans. Antennas Propag.*, Vol. 51, No. 7, 1516–1529, 2003.
17. Majid, H. A., M. K. A. Rahim, and T. Masri, "Microstrip antenna's gain enhancement using left-handed metamaterial structure," *Progress In Electromagnetics Research M*, Vol. 8, 235–247, 2009.